Journal of Computational Applied Mechanics 2025, 56(3): 587-601

DOI: 10.22059/jcamech.2025.392399.1415

RESEARCH PAPER

Comparative Study of Non-Isothermal Poiseuille Flow of Couple Stress Fluid in Reynolds Model Between Inclined Plates Using Two Homotopy-Based Methods

Muhammad Farooq [a], Rashid Nawaz [b], Alamgeer Khan [a], Faridoon Shahid [a], Ilker Ozsahin [c], Berna Uzun [c, d], Hijaz Ahmad [*, c, e]

[a] *Department of Mathematics, Abdul Wali Khan University, Mardan, KP, 23200, Pakistan*
[b] *UniSa STEM, University of South Australia*
[c] *Operational Research Center in Healthcare, Near East University, 99138, Nicosia/TRNC Mersin 10, Turkey*
[d] *Department of Mathematics, Faculty of Arts and Sciences, Near East University, 99138, Nicosia/TRNC Mersin 10, Turkey*
[e] *Department of Mathematics, College of Science, Korea University, 145 Anam-ro, Seongbuk-gu, Seoul 02841, South Korea*

Abstract

This work examines the Poiseuille flow of the Reynolds model's non-isothermal couple stress fluid between heated inclined plates. Using the Optimal Homotopy Asymptotic Method with DJ Polynomials (OHAM-DJ) and the Asymptotic Homotopy Perturbation method (AHPM), the strongly non-linear system of ordinary differential equations have been studied. The AHPM and OHAM-DJ have been used to approximate the results for the velocity profile, shear stress, temperature distributions, average velocity and volume flux. It is important to note that the outcomes obtained from these two methods closely resemble one another. In addition to being shown graphically, the impact of various factors on the flow problem have been investigated mathematically.

Keywords: Couple Stress Fluid, Optimal Homotopy Asymptotic Method, Asymptotic Homotopy, Perturbation method; Poiseuille Flow; Reynolds Model, Non-isothermal Poiseuille flow, Inclined plates

1. Introduction

Non-Newtonian liquids have a varied collection of applications in numerous scientific and technological domains, non-Newtonian fluids have become a very tempting alternative to Newtonian fluids for physicists, engineers, and mathematicians in recent decades [1-3]. The join stress liquid concept, which Stokes established, is one of the liquid concepts that have drawn a lot of attention from researchers and scientists [4]. Owing to the difficulty of these liquids, multiple constitutive models have remained advocated for various types of these liquids, as they cannot be accommodated into a solitary constitutive model. Due to the numerous beneficial uses of non-Newtonian fluids in contemporary skill and knowledge, numerous researchers have attempted to solve many non-Newtonian liquid movement problems. The impression of couple stress liquid arises owing to the procedure, that by which technique the fluid intermediate be modeled for the automated interactions. This hypothesis accurately describes the behaviour of fluids flowing through substructures, like as liquid crystals, lubricants, and animal blood,

* Corresponding author.: *E-mail address:* hijaz.ahmad@neu.edu.tr

containing polymer additives [5-10]. Amid the several fluid representations that are employed to clarify the performance of the non-Newtonian liquid, the pair stress fluid attracted a lot of interest. [11-14]. The fluids composed of unbending particles postponed in a viscous average with random orientation are defined by the couple stress fluids model. In certain fluids, the stress tensor is anti-symmetric. Therefore, classical Newtonian theory is unable to predict the precise flow behaviour of a fluid. The couple stress fluid model's key feature is that its solutions resemble Navier-Stokes equations. Because it is mathematically simpler than other fluid models, this model has been applied widely.

Various techniques have been employed in the literature to examine flow issues. These many approaches which serve as the primary instruments for researching flow problems include iterative, numerical, Homotopy-based techniques, and perturbation. Each of these approaches has benefits and drawbacks. Numerical techniques employ separation, which has an impact on exactness. The computing work and time required by the numerical methods were substantial. When there is significant non-linearity, numerical techniques cannot produce reliable findings. [15] Investigated both linear and non-linear functional equations using a novel technique. Its merging has stayed confirmed in [16]. Scholars in [17] dubbed this practice OHAM with DJ polynomials (OHAM-DJ) when they working DJM in OHAM to examine nonlinear differential equations.

In this work, two heated parallel inclined plates and their Poiseuille flow of incompressible pair stress fluid have been examined. The estimated results for the temperature, velocity, shear stress and average velocity on the plates have been derived using the OHAM-DJ and AHPM. This paper is divided into multiple sections. Basic governing equations are given in section 2. Problem construction is covered in piece 3, methods are introduced in piece 4, while solution of problem are assumed in piece 5, average velocity, volume flux and shear stress are delivered in piece 6, outcomes and debates are included in piece 7, and the work's conclusion is found in the final piece 8.

2. Basic Equations

The following are the equations for mass, momentum, and conservation of energy for an incompressible fluid [18, 19].

$$\nabla.\mathrm{Z} = 0, \tag{1}$$

$$\rho\dot{\mathrm{Z}} = \nabla.\tau - \eta\nabla^4\mathrm{Z} + \rho f, \tag{2}$$

$$\rho c_p\dot{\Theta} = \kappa\nabla^2\Theta + \tau L, \tag{3}$$

Velocity vector is represented by Z, τ is the gradient of the Cauchy stress tensor, the temperature is signified by Θ, signals constant density ρ. The couple stress parameter is represented by η in this case, the body force is represented by f, the specific heat is represented by c_p, and the material time derivative is represented by $\frac{D}{Dt}$ and given as below

$$\frac{D}{Dt}(\bullet) = \left(\frac{\partial}{\partial t} + \mathrm{Z}.\nabla\right)(\bullet). \tag{4}$$

Cauchy stress tensor is shown τ here as below.

$$\tau = -p\,I + \mu A_1. \tag{5}$$

First Rivilin-Ericksen tensor is symbolized by A_1, and given as follows, anywhere the unit tensor is signified by I, the dynamic pressure is signified by p, the coefficient of viscosity is represented by μ,

$$A_1 = L + L^t. \tag{6}$$

3. Formulation of Problem

Examine the steady Plane Poiseuille flow that exists between two infinitely parallel, inclining plates. Gravity and the constant pressure gradient force the fluid to move while both plates remain static. The temperatures of the lower and upper plates remain at and, Θ_0 and Θ_1. correspondingly. Figure 1 shows the coordinate system under

consideration. There is an angle of among the plates and the straight direction β. The μ viscosity varies with temperature Θ. The velocity and temperature are displayed as follows.

$$Z = Z(z,0,0),\ \Theta = \Theta(y)\ \ and\ z = z(y). \tag{7}$$

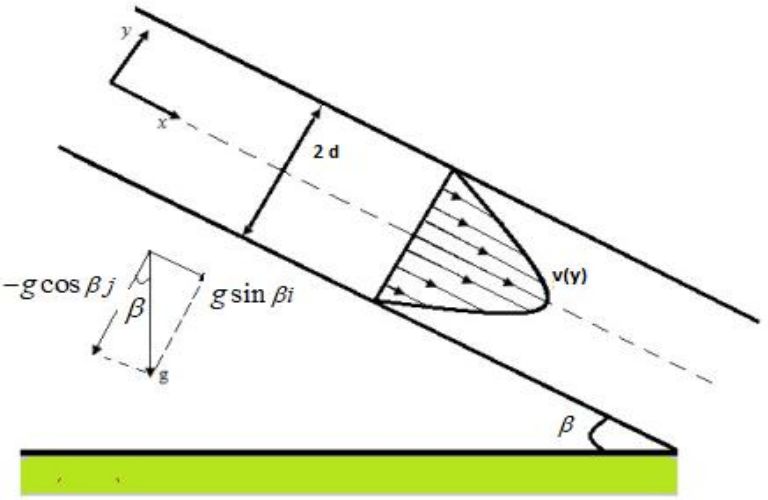

Figure 1: Geometry of the problem

By putting Eq. (7), Eq. (1) is satisfied identically. Additionally, Eq. (2) and (3) reduced to

$$\mu\frac{d^2z}{dy^2} - \eta\frac{d^4z}{dy^4} + \frac{d\mu}{dy}\frac{dz}{dy} - \frac{\partial p}{\partial x} + \rho g\sin\beta = 0, \tag{8}$$

$$\frac{d^2\Theta}{dy^2} + \frac{\eta}{\kappa}\left(\frac{d^2z}{dy^2}\right)^2 + \frac{\mu}{\kappa}\left(\frac{dz}{dy}\right)^2 = 0. \tag{9}$$

The boundaries of equations (8–9) are represented by equations (10–12).

$$z(d) = 0, z(-d) = 0, \tag{10}$$

$$z"(d) = 0, z"(-d) = 0, \tag{11}$$

$$\Theta(d) = \Theta_1,\ \Theta(-d) = \Theta_0. \tag{12}$$

Boundary conditions with no slip are represented by equation (10). It is clear from equation (11) that couple stress reduces at the plates. The dimensionless restrictions as a whole are:

$$\begin{aligned} &z^* = \frac{z}{Z}, y^* = \frac{y}{d}, \Theta^* = \frac{\Theta - \Theta_0}{\Theta_1 - \Theta_0}, x^* = \frac{x}{d}, p^* = \frac{p}{\mu_0 Z/d}, \mu^* = \frac{\mu}{\mu_0}, \\ &B_r = \frac{\mu_0 Z^2}{\kappa(\Theta_1 - \Theta_0)}, B^2 = \frac{\mu_0 d^2}{\eta}, G = -\frac{B^2 d^5}{\mu_0 Z}\frac{\partial p}{\partial x} + \frac{\rho g d^4}{\eta Z}\sin\beta. \end{aligned} \tag{13}$$

With boundary conditions (10)–(12) and removing the asterisks, equations (8)–(9) can be expressed as

$$\frac{d^4z}{dy^4} - B^2\frac{d\mu}{dy}\frac{dz}{dy} - B^2\mu\frac{d^2z}{dy^2} - G = 0, \tag{14}$$

$$\frac{d^2\Theta}{dy^2} + B_r\mu\left(\frac{dz}{dy}\right)^2 + \frac{B_r}{B^2}\left(\frac{d^2z}{dy^2}\right)^2 = 0, \tag{15}$$

$$z(1) = 0,\ z"(-1) = 0,\ z(-1) = 0,\ z"(1) = 0, \tag{16}$$

$$\Theta(-1) = 0,\ \Theta(1) = 1. \tag{17}$$

The Reynolds viscosity model is as shadows in its dimensionless.

$$\mu = \exp(-M\Theta). \tag{18}$$

Here, let's assume that $M = \in \mathrm{m}$ there $\in$ is a tiny parameter. By using equation (18)'s Taylor series expansion, one may obtain

$$\mu = 1 - \in \mathrm{m}\Theta, \frac{d\mu}{dy} \cong - \in \mathrm{m}\frac{d\Theta}{dy}. \tag{19}$$

4. Description of the methods

4.1. Basic Concept of OHAM-DJ

Suppose the differential equation

$$L(\eta(\pi)) + g(\pi) + G(\eta(\pi)) = 0,\ B(\eta, \frac{d\eta}{d\pi}) = 0. \tag{20}$$

Here $g(\pi)$ is the known function, here the linear operator is denoted by L, the unknown function is denoted by $\eta(\pi)$. B Is the boundary operator, non-linear operator is denoted by $G(\eta(\pi))$

By OHAM we have

$$(1-p)[L(\eta(\pi,p)) + g(\pi))] = D(p)[L(\eta(\pi,p)) + g(\pi)) + G(\eta(\pi,p))],$$

$$B\left(\eta(\pi,p), \frac{d\eta(\pi,p)}{d\pi}\right) = 0. \tag{21}$$

An embedding parameter is present and f $p \in [0,1]$ here, and the secondary function is represented by $D(p)$, so that for $p \neq 0$ $D(p)$ is non-zero or $p = 0$ that is $D(0) = 0,$ evident after $p = 0$ and $p = 1$ it generates

$$\eta(\pi,0) = \lambda_0(\pi),\ \eta(\pi,1) = \lambda(\pi). \tag{22}$$

The result $\eta(\pi,q)$ differs from $w_0(\pi)$ to $w(\pi)$, as p diverges from 0 to 1, the outcome $w_0(\pi)$ can be attained by putting $p = 0$ in Eq. (20).

$$L(\lambda_0(\pi)) + g(\pi) = 0,\ B(\lambda_0 \frac{d\lambda_0}{d\pi}) = 0. \tag{23}$$

One way to express the auxiliary function is as

$$D(p) = pc_1 + p^2c_2 + p^3c_3 + ...,. \tag{24}$$

Here c_i, $i = 1,2,3...$ are coefficients. Now let us income the answer of equation (21) in the arrangement

$$\eta(\pi, p, c_i) = \lambda_0(\pi) + \sum_{j\geq 1} \lambda_j(\pi, c_i)p^j. \qquad i = 1,2,... \tag{25}$$

The non-linear component $G(\eta(\pi, p))$ is broken down as

$$G = G(\lambda_0) + p[G(\lambda_0 + \lambda_1) - G(\lambda_0)] + p^2[G(\lambda_0 + \lambda_1 + \lambda_2) - G(\lambda_0 + \lambda_1)] + ... \tag{26}$$

Where (DJ) polynomials are represented as

$$G(\lambda_0),\ [G(\lambda_0 + \lambda_1) - G(\lambda_0)],\ [G(\lambda_0 + \lambda_1 + \lambda_2) - G(\lambda_0 + \lambda_1)],...$$

It was demonstrated by Sachin Bhalekar and Varsha Daftardar-Gejji in [16] that these polynomials converge. Simplified, it may be expressed as

$$\begin{aligned} G_0 &= G(\lambda_0), \\ G_1 &= G(\lambda_0 + \lambda_1) - G(\lambda_0), \\ G_2 &= G(\lambda_0 + \lambda_1 + \lambda_2) - G(\lambda_0 + \lambda_1), \end{aligned}$$

Consequently, in broad form as

$$G_n = \left(G\sum_{j=0}^{n} \lambda_j \right) - \left(G\sum_{j=0}^{n-1} \lambda_j \right) \tag{27}$$

$$G = G_0 + \sum_{j=0}^{n} p^k G_k \tag{28}$$

Putting (24), (25), (26) and (28) in (21) and matching similar powers of p the subsequent classification revenue

$$L(\lambda_0(\pi)) + g(\pi) = 0, \qquad B(\lambda_0 \frac{d\lambda_0}{d\pi}) = 0. \tag{29}$$

$$L(\lambda_1(\pi)) = c_1 G_0(\lambda_0(\pi)), \qquad B(\lambda_1 \frac{d\lambda_1}{d\pi}) = 0. \tag{30}$$

$$\begin{aligned} L(\lambda_j(\pi) - \lambda_{j-1}(\pi)) = c_j G_0(\lambda_0(\pi) + \sum_{k=1}^{j-1} c_k [L(\lambda_{j-k}(\pi)) \\ + G_{j-k}(\lambda_0(\pi), \lambda_1(\pi), ..., \lambda_{j-1}(\pi))], \end{aligned} \qquad B(\lambda_j \frac{d\lambda_j}{d\pi}) = 0.\ j = 1,2,... \tag{31}$$

The system of equations (23), (30) and (31), for $\lambda_j(\pi),\ j \geq 0$, can easily be solved. Equation (25)'s solution, or meeting, is entirely dependent on $c_1, c_2, c_3, ...$ At $p = 1$ if it is convergent, then equation (25) indicates

$$\eta(\pi, c_k) = \lambda_0(\pi) + \sum_{j\geq 1} \lambda_j(\pi, c_k). \tag{32}$$

Typically, the outcome of equation (20) is roughly represented by

$$\eta^n(\pi, c_l) = \lambda_0(\pi) + \sum_{j=1}^{n} \lambda_j(\pi, c_l),\ l = 1,2,...n. \tag{33}$$

After putting equation (33) in equation (20) residual converts

$$R(\pi, c_l) = L(\eta^n(\pi, c_l)) + g(\pi) + G(\eta^n(\pi, c_l)),\ l = 1, 2, ..., n. \tag{34}$$

The exact answer $\eta^n(\pi, c_k)$ is found if $R(\pi, c_k) = 0$ the remaining is equivalent to zero. However, if $R(\pi, c_k) \neq 0,$ it may be reduced as follows

$$J(c_k) = \int_a^b R^2(\pi, c_k) d\pi. \tag{35}$$

Where the constants a and b represent the boundary of integral, which depends on the problem being studied. Additionally, the following condition can be used to evaluate constants $c_1, c_2, c_3, ...$

$$\frac{\partial J}{\partial c_i} = 0, \qquad i = 1, 2, ..., n. \tag{36}$$

Equation (33), after these constants' values are obtained, provides an approximate solution.

4.2. Basic Idea of AHPM

AHPM is explained in this subsection; let's look at the differential equation.

$$L(\eta(\Im)) + f(\Im) + N(\eta(\Im)) = 0 \tag{37}$$

Where $f(\Im)$ is known function, the linear operator is epitomized by L, the unknown function is indicated by $\eta(\Im)$, here the nonlinear operator is indicated by $N(\eta(\Im))$. Consider the homotopy $\psi(\Im, p) : \Omega \times [0,1] \to R$ [24] such that

$$L(\psi(\Im, p)) + f(\Im) - p[N(\psi(\Im, p))] = 0, \tag{38}$$

wherever the constraint for embedding $p \in [0,1]$. An alternative version of the deformation equation OHAM, first forth by [22], is represented by equation (38) as shadows.

$$(1-p)[L(\psi(\Im, p)) + f(\Im))] - H(p)[L(\psi(\Im, p)) + f(\Im)) + N(\psi(\Im, p))] = 0, \tag{39}$$

obviously when $p = 0$ and $p = 1$ it yields

$$\psi(\eta(\Im, 0)) = \lambda_0(\Im),\ \psi(\eta(\Im, 1)) = \lambda(\Im),$$

Consider $\psi(\eta(\Im, p))$ is in the form

$$\psi(\eta(\Im, p)) = v_0(\Im) + \sum_{j=1}^{\infty} v_j(\Im) p^j, \tag{40}$$

the non-linear part $N(\psi(\pi, p))$ is as under

$$N(\psi(\Im, p)) = Q_1 N_0 + \sum_{j=1}^{\infty} \left(\sum_{n=0}^{j} Q_{j+1-n} N_n \right) p^j,\ Q_1 + Q_2 + Q_3 + ... = -1, \tag{41}$$

where

$$Q_j = Q_j(\Im, c_j),\ \mathrm{j} = 1, 2, 3, ... \tag{42}$$

We obtain by replacing (40) and (41) in (38) and comparing like powers of

$$p^0 : L(\lambda_0(\Im)) + f(\Im) = 0,$$
$$p^1 : L(\lambda_1(\Im)) = Q_1 N_0,$$
$$p^2 : L(\lambda_2(\Im)) = Q_2 N_0 + Q_1 N_1,$$
$$p^3 : L(\lambda_3(\Im)) = Q_3 N_0 + Q_2 N_1 + Q_1 N_2,$$

thus, in general

$$p^l : L(\lambda_l(\Im)) = \sum_{j=0}^{l-1} Q_{l-j} N_j.$$

The equation (38) at $r = 1$ touches to the exact resolution of equation (37), explicitly

$$\eta(\Im, c_k) = \lambda_0(\Im) + \sum_{j=1}^{\infty} \lambda_j(\Im, c_k), k = 1, 2, 3... \tag{43}$$

Equation (43) is substituted for equation (37) and residual becomes

$$R(\Im, c_k) = L(\eta\ (\Im, c_k)) + f(\Im) + N(\eta(\Im, c_k)),\ k = 1, 2, ..., n. \tag{44}$$

The particular answer $\eta^n(\Im, c_k)$ is got if $R(\Im, c_k) = 0$, the residual is identical to zero. However, if $R(\Im, c_k) \neq 0,$ it may be reduced as follows

$$J(c_k) = \int_a^b R^2(\pi, c_k) d\pi. \tag{45}$$

Where the constants a and b represent the boundary of the integral, which depends on the problem being studied. Additionally, the following condition can be used to evaluate constants $c_1, c_2, c_3, ...$

$$\frac{\partial J}{\partial c_i} = 0, \qquad i = 1, 2, ..., n. \tag{46}$$

Equation (43), once these constants' values are obtained, provides an approximate solution.

5. The solution to the Problem

Zero order OHAM-DJ results for velocity and temperature distributions

Zero order velocity problem

$$z_0''''(y) - G = 0,$$
$$z_0(-1) = 0,\ z_0(1) = 0,\ z_0''(-1) = 0,\ z_0''(1) = 0.$$

Zero order velocity solution

$$z_0 = \frac{1}{24}(5 - 6y^2 + y^4).$$

First order velocity problem

$$G - B^2 m\varepsilon c_1 z_0'(y)\Theta_0'(y) + B^2 c_1 z_0''(y) - B^2 m\varepsilon c_1 z_0''(y)\Theta_0(y)$$
$$-(1 + c_1) z_0''''(y) + z_1''''(y) = 0,$$
$$z_1(-1) = 0,\ z_1(1) = 0,\ z_1''(-1) = 0,\ z_1''(1) = 0.$$

First order velocity solution

$$z_1 = \frac{1}{10080}(-0.000112 + 3.8\times10^{-20}\ y + 2.0\times10^{-3}\ y^2 - 5.7\times10^{-20} y^3 - 2.2\times10^{-5}\ y^4 + 2.2\times10^{-20} y^5 + 1.2\times10^{-13} y^6 - 2.1\times10^{-21}\ y^7).$$

OHAM-DJ solutions of velocity profile (Z_o) up to first order

$$Z_o = z_0 + z_1$$

$$Z_O = 1/24\ (5 - 6\ y^2 + y^4) + 1/10080(-0.000112 + 3.8\times10^{-20}\ y + 2.0\times10^{-3}\ y^2 - 5.7\times10^{-20} y^3 - 2.2\times10^{-5} y^4 + 2.2\times10^{-20} y^5 + 1.2\times10^{-13} y^6 - 2.1\times10^{-21}\ y^7). \quad (47)$$

OHAM-DJ results of temperature distributions (Θ_o) up to first order

The related boundary conditions and the zero component equations for temperature are

$$\Theta_0''(y) = 0,$$

$$\Theta_0(-1) = 0,\ \Theta_0(1) = 1.$$

Zero order solution of temperature

$$\Theta_0 = \frac{1}{2}(1 + y).$$

The related boundary conditions and the first component equations for temperature are

$$-B_r c_1 (z_0'(y))^2 + m\varepsilon B_r c_1 \Theta_0 (z_0'(y))^2 - \frac{B_r c_1 (z_0''(y))^2}{B^2} - (1 + c_1)\Theta_0''(y) + \Theta_1''(y) = 0,$$

$$\Theta_1(-1) = 0,\ \Theta_1(1) = 0.$$

First order temperature solution

$$\Theta_1 = 34.4(3.2 - 1.5\times10^{-15} y - 4.3\ y^2 + 1.4\ y^4 - 0.3 y^6 - 6.6\times10^{-16} y^7 + 2.1\times10^{-15} y^5 + 6.4\times10^{-17} y^9 - 2.7\times10^{-9} y^8).$$

$$\Theta_O = \Theta_0 + \Theta_1.$$

$$\Theta_O = \frac{1}{2}(1 + y) + (3.2 - 1.5\times10^{-15} y - 4.3\ y^2 + 2.1\times10^{-15} y^5 + 1.4\ y^4 - 0.3 y^6 - 2.7\times10^{-9} y^8 - 6.6\times10^{-16} y^7 + 6.4\times10^{-17} y^9)34.4. \quad (48)$$

The following are AHPM's first-order solutions for velocity profile (Z_A) and temperature distributions (Θ_A)

Zero order velocity problem

$$z_0''''(y) - G = 0,$$

$$z_0(-1) = 0,\ z_0(1) = 0,\ z_0''(-1) = 0,\ z_0''(1) = 0.$$

Zero order velocity solution

$$z_0 = \frac{1}{24}(5 - 6\ y^2 + y^4).$$

First order velocity problem

$$z_1''''(y) + c_1 N_0 = 0,$$

$$N_0 = -B^2(1-m\,\varepsilon\,\Theta_0(\mathrm{y}))z_0^{''}(y) - B^2 m\,\varepsilon\Theta_0^{'}(y)\,z_0^{'}(y)),$$

$$z_1(-1)=0,\ z_1(1)=0,\ z_1^{''}(-1)=0,\ z_1^{''}(1)=0.$$

First order velocity solution

$$\begin{aligned} z_1 = \frac{1}{10080}(&-0.0001 + 7.1\times10^{-13}\ \mathrm{y} + 1.6\times10^{-4}\ y^2 \\ &- 1.1\times10^{-12}\ y^3 - 3.4\times10^{-5}\,y^4 + 4.0\times10^{-13}\,y^5 \\ &+ 2.2\times10^{-6}\,y^6 - 3.8\times10^{-14}\,y^7). \end{aligned}$$

$$\mathrm{Z}_A = z_0 + z_1.$$

$$\begin{aligned} \mathrm{Z}_A = (5 &- 6\,y^2 + y^4)/24 + (-0.0001 + 7.1\times10^{-13}\,y + 1.6\times10^{-4}\ y^2 \\ &- 1.1\times10^{-12}\ y^3 - 3.4\times10^{-5}\,y^4 + 4.0\times10^{-13}\,y^5 \\ &+ 2.2\times10^{-6}\,y^6 - 3.8\times10^{-14}\,y^7)/10080. \end{aligned} \tag{49}$$

AHPM's solutions of temperature (Θ_A)

Zero order problems of temperature is

$$\Theta_0^{''}(\mathrm{y}) = 0,$$
$$\Theta_0(-1)=0,\ \Theta_0(1)=1.$$

Zero order solution of temperature is

$$\Theta_0 = \frac{1}{2}(1+\mathrm{y}).$$

First order problem of temperature is

$$\Theta_1^{''}(\mathrm{y}) + c_1 N_0 = 0,$$

$$N_0 = B_r(1-\varepsilon m\Theta_0)(z_0^{'}(y))^2 + \frac{B_r}{B^2}(z_0^{''}(y))^2,$$

$$\Theta_1(-1)=0,\ \Theta_1(1)=0.$$

First order temperature solution

$$\begin{aligned} \Theta_1 = 34.4\,(&8.3 - 3.8\times10^{-15}\ \mathrm{y} + 5.4\times10^{-15}\,y^5 - -11.3\,y^2 \\ &+ 3.8\,y^4\,7.5\times10^{-1}\,y^6 - 7.2\times10^{-9}\,y^8 - 1.7\times10^{-15}\,y^7 \\ &+ 1.7\times10^{-16}\ y^9). \end{aligned}$$

$$\Theta_A = \Theta_0 + \Theta_1$$

$$\begin{aligned} \Theta_A = (1 &+ y)/2 + 34.4\,(8.3 - 3.8\times10^{-15}\,y - 7.5\times10^{-1}\,y^6 \\ &+ 5.4\times10^{-15}\,y^5 - 11.3\,y^2 + 3.8\,y^4 - 1.7\times10^{-15}\,y^7 - 7.2\times10^{-9}\,y^8 \\ &+ 1.7\times10^{-16}\,y^9). \end{aligned} \tag{50}$$

6. Volume Flux, Average Velocity, Shear Stress

6.1. Volume Flux

The formula for volume flux is as follow:

$$Q = \int_{-1}^{1} \mathrm{Z}\,dy. \tag{51}$$

Equations (47) and (49) can be substituted in (44) to indicate

$$Q_O = 2.8\times10^{-9} B^2 G m\epsilon + 0.26\ \mathrm{G} - 5.7\times10^{-9}\ B^2 G. \tag{52}$$

$$Q_A = 0.1\ B^2\ \mathrm{G\ m}\ \epsilon + \frac{4G}{15} - 0.1\ B^2 \mathrm{G}\ . \tag{53}$$

6.2. Average Velocity

The average velocity is represented by and is described as follows:

$$\overline{\mathrm{Z}} = \frac{Q}{d}. \tag{54}$$

Equation (54) in dimensionless form agrees by the movement amount provided in equations (52) and (53).

6.3. Shear Stress

In dimensionless form the shear stress is represented and clear as under

$$t_{\mathrm{p}} = -\mu\, D\left[\mathrm{Z}, y\right], y = 1. \tag{55}$$

$$\mathrm{t}_{\rho O} = -\left(-\frac{G}{3} + \frac{1}{10080}\left(0.0001792\ \mathrm{G} + 0.00007168\ \mathrm{B^2G} - 0.0000401067\ \mathrm{B^2G\ m}\ \varepsilon\right)\right)\mu. \tag{56}$$

$$\mathrm{t}_{\rho A} = -\left(-\frac{G}{3} + \frac{1}{10080}\left(1343.99\ \mathrm{B^2G} - 751.995\ \mathrm{B^2G\ m}\ \varepsilon\right)\right)\mu. \tag{57}$$

The superior plate is fronting the coordinate system's negative $y-\mathrm{direction}$, which is why there is a minus symbol [23]. $\mathrm{Q_O}$, Q_A, $\mathrm{t}_{\rho O}$ and $\mathrm{t}_{\rho A}$ The shear stresses and volume fluxes in this case were determined via AHPM and OHAM-DJ, respectively.

7. Results and Discussion

In this paper, the Poiseuille flow between two inclined plates has been studied using two homotopy-based approaches (AHPM and OHAM-DJ). Using both of these methods, the velocity also temperature difference for various parameters, such as B, m, G, B_r and ε, have been studied. Temperature distributions, velocity profiles, and the matching residuals for both approaches are provided in tables 1-2. Table 3 shows the absolute variations in the temperature distributions and velocity profiles for the two approaches for various parameter values G, B, m, B_r and ε. Figures (2–5) show how various parameters G, B, m, B_r and ϵ affect the distributions of temperature and velocity. The velocity profiles of OHAM-DJ and AHPM are compared for various parameters in figures (2–3), and they show great agreement. These figures make it obvious that both approaches' velocities are parabolic. As can be seen from these graphs, the temperature of the fluid was examined for various parameters in figures (4-5) using both approaches, and the results showed great similarity. Both approaches have been used to investigate the volumetric flow rate for a range of factors, and the results are in good agreement, as figures (6-7) demonstrate. Using both approaches, the shear stress is examined for a range of parameters and is found to be very comparable, as shown in figures (8–9). Shear stress τ_p and parameter G both are in direct connection as perfect from these data.

Table 1: For $\varepsilon = 0.0003, G = 0.5,\ B = 0.0001,\ B_r = 0.0004$ and $m = 0.0002$.

y	OHAM-DJ (Z_0)	Residual (Z_0)	OHAM-DJ (Θ_O)	Residual (Θ_O)
-1.	-5.3×10^{-26}	-1.66667×10^{-9}	4.2×10^{-14}	1.42193×10^{-13}
-0.9	1.6×10^{-2}	-1.19167×10^{-9}	50.9488	2.55224×10^{-8}
-0.8	3.27×10^{-2}	-7.66667×10^{-10}	101.507	6.99766×10^{-8}
-0.7	4.8×10^{-2}	-3.91667×10^{-10}	150.799	1.0208×10^{-7}
-0.6	6.2×10^{-2}	-6.66665×10^{-11}	197.592	1.08393×10^{-7}
-0.5	74×10^{-2}	2.08333×10^{-10}	240.471	8.80076×10^{-8}
-0.4	8.5×10^{-2}	4.33333×10^{-10}	277.986	4.79471×10^{-8}
-0.3	9.3×10^{-2}	6.08333×10^{-10}	308.78	-7.34879×10^{-10}
-0.2	9.9×10^{-2}	7.33333×10^{-10}	331.69	-4.61336×10^{-8}
-0.1	0.102919	8.08333×10^{-10}	345.827	-7.79771×10^{-8}
0.	0.104167	8.33333×10^{-10}	350.636	-8.93945×10^{-8}
0.1	0.102919	8.08333×10^{-10}	345.927	-7.79771×10^{-8}
0.2	0.0992	7.33333×10^{-10}	331.89	-4.6133×10^{-8}
0.3	0.0930854	6.08333×10^{-10}	309.08	-7.3478×10^{-10}
0.4	0.0847	4.33333×10^{-10}	278.386	4.79468×10^{-8}
0.5	0.0742187	2.08333×10^{-10}	240.971	8.80078×10^{-8}
0.6	0.0618667	-6.66667×10^{-10}	198.192	1.08393×10^{-7}
0.7	0.0479187	-3.91667×10^{-10}	151.499	1.0208×10^{-7}
0.8	0.0327	-7.66667×10^{-10}	102.307	6.99769×10^{-8}
0.9	0.0165854	-1.19167×10^{-9}	51.8488	2.55224×10^{-8}
1.	-5.2519×10^{-26}	-1.66667×10^{-9}	1.	9.92803×10^{-15}

Table 2: For $m = 0.0002, G = 0.5,\ B_r = 0.0004, B = 0.0001,$ and $\varepsilon = 0.0003$.

y	AHPM (Z_A)	Residual (Z_A)	AHPM (Θ_A)	Residual (Θ_A)
-1.	-4.8×10^{-27}	1.33331×10^{-13}	-7.64869×10^{-14}	-2.91937×10^{-14}
-0.9	0.016585	1.37057×10^{-13}	133.305	1.08081×10^{-7}
-0.8	0.03270	1.27869×10^{-13}	265.588	2.96368×10^{-7}
-0.7	0.047918	1.06927×10^{-13}	394.554	4.32345×10^{-7}
-0.6	0.061866	7.66364×10^{-14}	516.979	4.59085×10^{-7}
-0.5	0.074218	4.04687×10^{-14}	629.156	3.72744×10^{-7}
-0.4	0.08470	2.58757×10^{-15}	727.292	2.03062×10^{-7}
-0.3	0.093085	-3.26415×10^{-14}	807.831	-3.13252×10^{-9}
-0.2	0.0992	-6.11625×10^{-14}	867.728	-1.95422×10^{-7}
-0.1	0.102919	-7.9698×10^{-14}	904.658	-3.30299×10^{-7}
0.	0.104167	-8.61218×10^{-14}	917.167	-3.78658×10^{-7}
0.1	0.102919	-7.9698×10^{-14}	904.758	-3.30299×10^{-7}
0.2	0.0992	-6.11625×10^{-14}	867.928	-1.95422×10^{-7}
0.3	0.093085	-3.26415×10^{-14}	808.131	-3.13165×10^{-9}
0.4	0.0847	2.58757×10^{-15}	727.692	2.03062×10^{-7}
0.5	0.074218	4.04687×10^{-14}	629.656	3.72744×10^{-7}
0.6	0.061866	7.66364×10^{-14}	517.579	4.59085×10^{-7}
0.7	0.0479187	1.06927×10^{-13}	395.254	4.32346×10^{-7}
0.8	0.0327	1.27869×10^{-13}	266.388	2.96368×10^{-7}
0.9	0.0165854	1.37057×10^{-13}	134.205	1.08082×10^{-7}
1.	-5.424×10^{-27}	1.33331×10^{-13}	1.	2.83172×10^{-13}

Table 3: For $G=0.9,\ \epsilon=0.09,\ m=1.2,\ B_r=0.9$ and $B=0.6.$

y	OHAM DJ (Z_O)	AHPM (Z_A)	Difference	OHAM-DJ (Θ_O)	AHPM (Θ_A)	Difference
-1	-1.387×10^{-17}	-1.105×10^{-17}	0	1.041×10^{-17}	-2.440×10^{-17}	0
-0.8182	0.0536797	0.0463047	0.007375	0.111749	0.145484	0.033735
-0.6162	0.107473	0.0926519	0.014821	0.233894	0.301841	0.067947
-0.4142	0.150002	0.129246	0.020756	0.352185	0.448111	0.095926
-0.2122	0.177445	0.152851	0.024594	0.464686	0.57922	0.114534
-0.0102	0.187477	0.16151	0.025967	0.569949	0.69138	0.121431
0.0102	0.187477	0.161515	0.025962	0.580146	0.701573	0.121427
0.2122	0.177445	0.152953	0.024492	0.676829	0.791272	0.114443
0.4142	0.150002	0.129407	0.020595	0.766278	0.862031	0.095753
0.6162	0.107473	0.0928115	0.014662	0.849958	0.917685	0.067727
0.8182	0.0536797	0.0463992	0.007281	0.92984	0.963398	0.033558
1	-1.387×10^{-17}	-1.105×10^{-17}	0	1.	1.	0

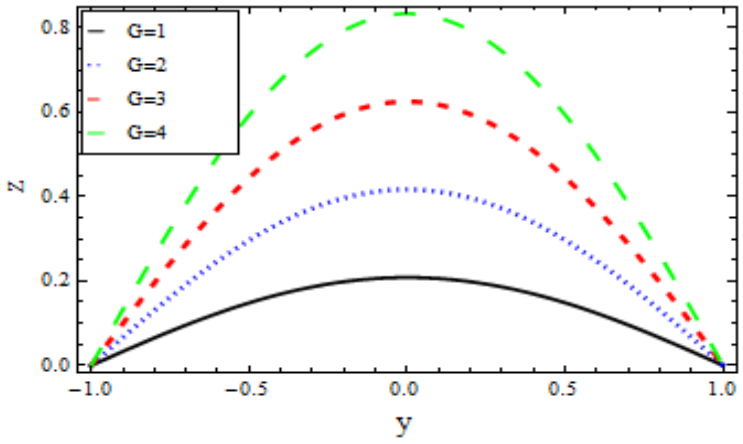

Figure 1: Velocity profile for $B_r=0.3,\ \epsilon=0.002,\ B=0.2$ and $m=0.0003$ using OHAM-DJ.

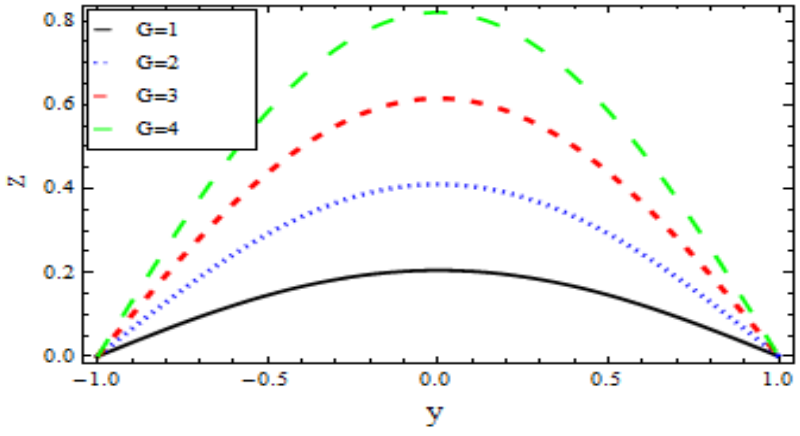

Figure 2: Velocity profile for $\epsilon=0.002, B=0.2, B_r=0.3$ and $m=0.0003$ using AHPM.

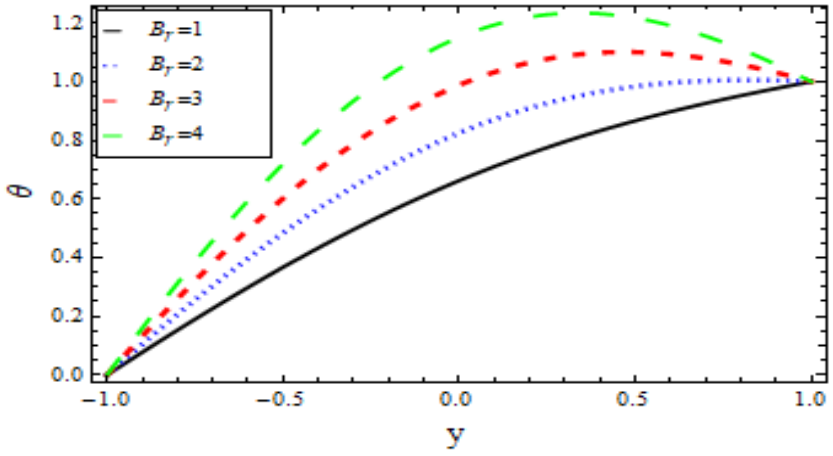

Figure 4: Temperature distributions for $B = 1, \varepsilon = 1,\ m = 0.1$ and $G = 2$ by OHAM-DJ.

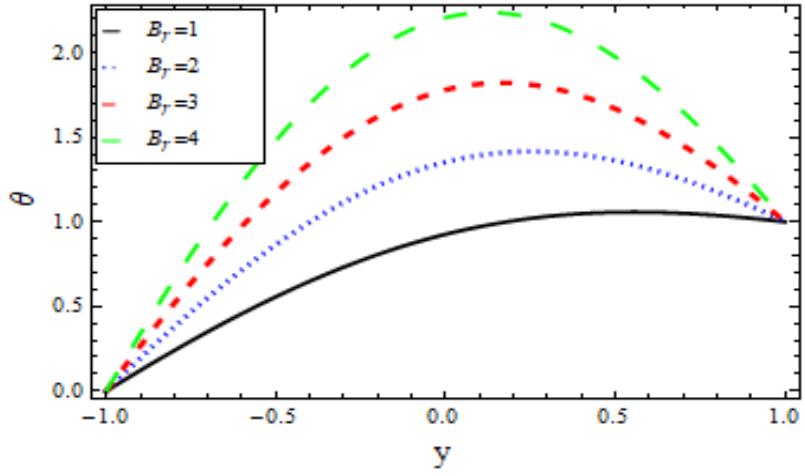

Figure 5: Temperature distributions for $\mathrm{m} = 0.1,\ \mathrm{G} = 2,\ \varepsilon = 1$ and $\mathrm{B} = 1$ by AHPM.

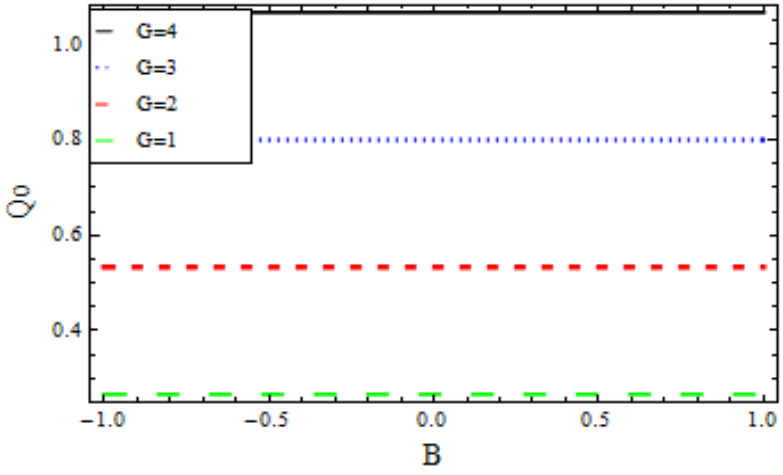

Figure 6: By OHAM-DJ variation in volume flux for $m = 3,\ \epsilon = 0.1$.

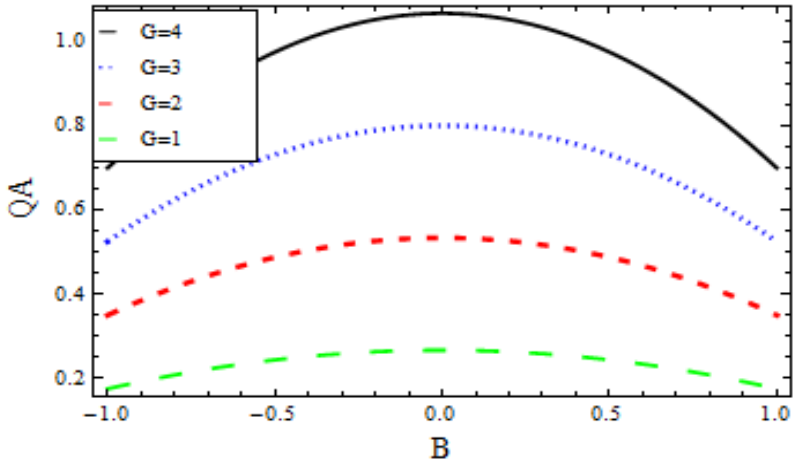

Figure 7: By AHPM variation in volume flux for $m=3,\ \epsilon=0.1.$

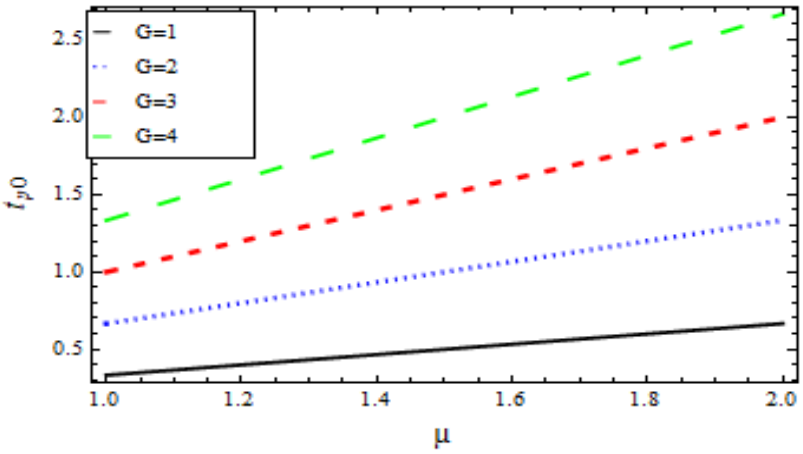

Figure 8: Shear stress variation for $B=1,\ \epsilon=0.1$ and $m=3$ by OHAM-DJ.

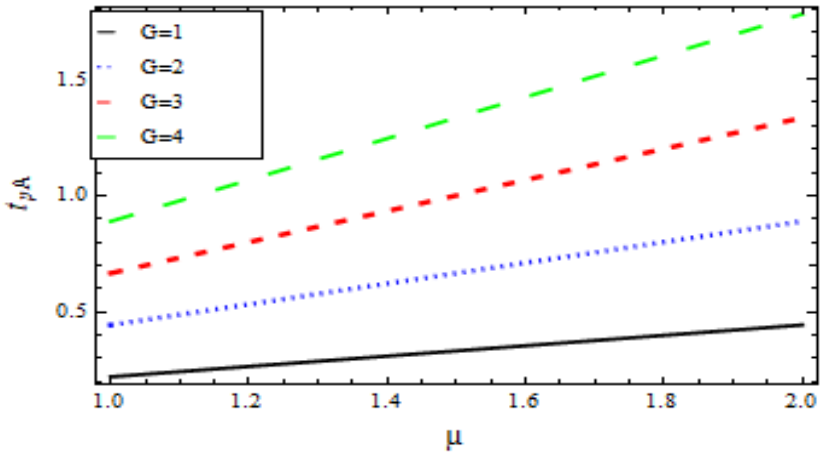

Figure 9: Shear stress variation for $m=3,\ \epsilon=0.1$ and $B=1$ by AHPM.

8. Conclusion

The current work presents a relative study of the pair stress fluids' steady Poiseuille flow among dual in similar inclined Reynolds model plates. The extremely nonlinear differential equations of couple stress fluids for temperature distribution, velocity, shear stress, and average velocity have been studied using OHAM-DJ and AHPM

methodologies. Both approaches' approximations for the volumetric flow rate, velocity, temperature distributions, and shear stress are shown mathematically and clearly, and it is discovered that they closely resemble each other.

References

[1] C. Fetecau, C. Fetecau, Decay of a potential vortex in an Oldroyd-B fluid, *International Journal of Engineering Science,* Vol. 43, No. 3-4, pp. 340-351, 2005.

[2] C.-I. Chen, C.-K. Chen, Y.-T. Yang, Unsteady unidirectional flow of an Oldroyd-B fluid in a circular duct with different given volume flow rate conditions, *Heat and Mass transfer,* Vol. 40, pp. 203-209, 2004.

[3] W. Tan, T. Masuoka, Stokes' first problem for a second grade fluid in a porous half-space with heated boundary, *International Journal of Non-Linear Mechanics,* Vol. 40, No. 4, pp. 515-522, 2005/05/01/, 2005.

[4] V. K. Stokes, 2012, *Theories of fluids with microstructure: An introduction*, Springer Science & Business Media,

[5] M. Devakar, T. Iyengar, Run up flow of a couple stress fluid between parallel plates, *Nonlinear Analysis: Modelling and Control,* Vol. 15, No. 1, pp. 29-37, 2010.

[6] S. Asghar, M. R. Mohyuddin, T. Hayat, Unsteady flow of a third-grade fluid in the case of suction, *Mathematical and computer modelling,* Vol. 38, No. 1-2, pp. 201-208, 2003.

[7] T. Hayat, M. Khan, M. Ayub, On the explicit analytic solutions of an Oldroyd 6-constant fluid, *International Journal of Engineering Science,* Vol. 42, No. 2, pp. 123-135, 2004.

[8] T. Hayat, R. Ellahi, F. Mahomed, Exact solutions for Couette and Poiseuille flows for fourth grade fluids, *Acta Mechanica,* Vol. 188, No. 1, pp. 69-78, 2007.

[9] A. Siddiqui, M. Ahmed, S. Islam, Q. Ghori, Homotopy analysis of Couette and Poiseuille flows for fourth grade fluids, *Acta mechanica,* Vol. 180, pp. 117-132, 2005.

[10] V. Daftardar-Gejji, H. Jafari, An iterative method for solving nonlinear functional equations, *Journal of mathematical analysis and applications,* Vol. 316, No. 2, pp. 753-763, 2006.

[11] S. Bhalekar, V. Daftardar-Gejji, Convergence of the new iterative method, *International journal of differential equations,* Vol. 2011, No. 1, pp. 989065, 2011.

[12] Z. Shah, R. Nawaz, S. Shah, S. Shah, M. Shah, Use of the Daftardar–Jafari polynomials in optimal homotopy asymptotic method for the solution of linear and nonlinear Klein–Gordon equations, *Journal of Applied Environmental and Biological Sciences,* Vol. 6, pp. 71-81, 2016.

[13] S. Islam, C. Zhou, Exact solutions for two dimensional flows of couple stress fluids, *Zeitschrift für angewandte Mathematik und Physik,* Vol. 58, No. 6, pp. 1035-1048, 2007.

[14] S. Islam, I. Ali, X. Ran, A. Shah, A. Siddiqui, Effects of couple stresses on Couette and Poiseuille flow, *Int. J. Nonlinear Sci. Numer. Simmul,* Vol. 10, No. 1, pp. 99-112, 2009.

[15] T. Chinyoka, O. D. Makinde, Analysis of transient generalized Couette flow of a reactive variable viscosity third-grade liquid with asymmetric convective cooling, *Mathematical and Computer Modelling,* Vol. 54, No. 1-2, pp. 160-174, 2011.

[16] Y. Aksoy, M. Pakdemirli, Approximate analytical solutions for flow of a third-grade fluid through a parallel-plate channel filled with a porous medium, *Transport in Porous Media,* Vol. 83, pp. 375-395, 2010.

[17] V. Marinca, N. Herişanu, Application of optimal homotopy asymptotic method for solving nonlinear equations arising in heat transfer, *International communications in heat and mass transfer,* Vol. 35, No. 6, pp. 710-715, 2008.

[18] T. Papanastasiou, G. Georgiou, A. N. Alexandrou, 2021, *Viscous fluid flow*, CRC press,

[19] A. Siddiqui, M. Ahmed, Q. Ghori, Couette and Poiseuille flows for non-Newtonian fluids, *International Journal of Nonlinear Sciences and Numerical Simulation,* Vol. 7, No. 1, pp. 15-26, 2006.